Title

Estimating peak skin and eye lens dose from neuroperfusion examinations: Use of Monte Carlo based simulations and comparisons to CTDIvol, AAPM Report No. 111, and ImPACT dosimetry tool values

Journal

Medical Physics, 40(9)

ISSN

0094-2405

Authors

Zhang, Di
Cagnon, Chris H
Villablanca, J Pablo
et al.

Publication Date

2013-09-01

DOI

10.1118/1.4816652

Peer reviewed

Estimating peak skin and eye lens dose from neuroperfusion examinations: Use of Monte Carlo based simulations and comparisons to $CTDI_{vol}$, AAPM Report No. 111, and ImPACT dosimetry tool values

Di Zhang[a)]
Toshiba America Medical Systems, 2441 Michelle Drive, Tustin, California 92780 and UCLA David Geffen School of Medicine, Westwood Medical Plaza, Los Angeles, California 90025

Chris H. Cagnon and J. Pablo Villablanca
UCLA David Geffen School of Medicine, Westwood Medical Plaza, Los Angeles, California 90025

Cynthia H. McCollough
Radiology, Mayo Clinic, East 2 Mayo Building, 200 1st Street Southwest, Rochester, Minnesota 55905

Dianna D. Cody
Diagnostic Imaging Physics, U.T.M.D Anderson Cancer Center, 1515 Holcombe Boulevard Unit 56, Houston, Texas 77030

Maria Zankl
German Research Center for Environmental Health (GmbH), Ingolstädter Landstreet 1, 85764 Neuherberg, Germany

John J. Demarco and Michael F. McNitt-Gray
UCLA David Geffen School of Medicine, Westwood Medical Plaza, Los Angeles, California 90025

(Received 20 April 2013; revised 8 July 2013; accepted for publication 11 July 2013; published 5 August 2013)

Purpose: CT neuroperfusion examinations are capable of delivering high radiation dose to the skin or lens of the eyes of a patient and can possibly cause deterministic radiation injury. The purpose of this study is to: (a) estimate peak skin dose and eye lens dose from CT neuroperfusion examinations based on several voxelized adult patient models of different head size and (b) investigate how well those doses can be approximated by some commonly used CT dose metrics or tools, such as $CTDI_{vol}$, American Association of Physicists in Medicine (AAPM) Report No. 111 style peak dose measurements, and the ImPACT organ dose calculator spreadsheet.
Methods: Monte Carlo simulation methods were used to estimate peak skin and eye lens dose on voxelized patient models, including GSF's Irene, Frank, Donna, and Golem, on four scanners from the major manufacturers at the widest collimation under all available tube potentials. Doses were reported on a per 100 mAs basis. $CTDI_{vol}$ measurements for a 16 cm CTDI phantom, AAPM Report No. 111 style peak dose measurements, and ImPACT calculations were performed for available scanners at all tube potentials. These were then compared with results from Monte Carlo simulations.
Results: The dose variations across the different voxelized patient models were small. Dependent on the tube potential and scanner and patient model, $CTDI_{vol}$ values overestimated peak skin dose by 26%–65%, and overestimated eye lens dose by 33%–106%, when compared to Monte Carlo simulations. AAPM Report No. 111 style measurements were much closer to peak skin estimates ranging from a 14% underestimate to a 33% overestimate, and with eye lens dose estimates ranging from a 9% underestimate to a 66% overestimate. The ImPACT spreadsheet overestimated eye lens dose by 2%–82% relative to voxelized model simulations.
Conclusions: $CTDI_{vol}$ consistently overestimates dose to eye lens and skin. The ImPACT tool also overestimated dose to eye lenses. As such they are still useful as a conservative predictor of dose for CT neuroperfusion studies. AAPM Report No. 111 style measurements are a better predictor of both peak skin and eye lens dose than $CTDI_{vol}$ and ImPACT for the patient models used in this study. It should be remembered that both the AAPM Report No. 111 peak dose metric and $CTDI_{vol}$ dose metric are dose indices and were not intended to represent actual organ doses. © *2013 American Association of Physicists in Medicine*. [http://dx.doi.org/10.1118/1.4816652]

Key words: computed tomography, radiation dose, Monte Carlo, neuroperfusion

1. INTRODUCTION

With the development of multidetector CT (MDCT) and increased computing power, CT perfusion (CTP) imaging has become a common clinical examination to identify deficits in cerebrovascular physiology in the setting of ischemic stroke. Rather than revealing cerebrovascular morphology, CTP provides important indices of cerebral hemodynamics, including

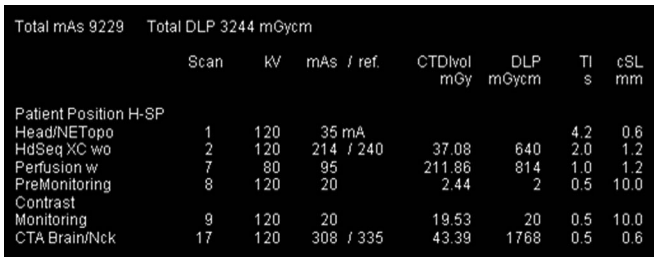

Total mAs 9229 Total DLP 3244 mGycm

	Scan	kV	mAs / ref.	CTDIvol mGy	DLP mGycm	TI s	cSL mm
Patient Position H-SP							
Head/NETopo	1	120	35 mA			4.2	0.6
HdSeq XC wo	2	120	214 / 240	37.08	640	2.0	1.2
Perfusion w	7	80	95	211.86	814	1.0	1.2
PreMonitoring	8	120	20	2.44	2	0.5	10.0
Contrast Monitoring	9	120	20	19.53	20	0.5	10.0
CTA Brain/Nck	17	120	308 / 335	43.39	1768	0.5	0.6

FIG. 1. An example of a dose report for a brain perfusion scan showing $CTDI_{vol}$ and DLP values for each individual scan series.

qualitative and quantitative relative cerebral blood flow, blood volume, and mean transit time. As a result, CTP has become an important noninvasive imaging technique for determining tissue state in patients with ischemic stroke. The information provided by CTP imaging can be used to confirm that a neurologic deficit is due to an underlying cerebral perfusion deficit, to determine the probable cause of the perfusion abnormality, and to help select from several treatment options within a critical and narrow time window.[1]

Because the radiation dose from routine head CT scans is relatively low (in the order of tens of mGy), potential stochastic effects have been considered the main concern in terms of the biological consequences from radiation dose. However, during CT perfusion imaging, the patient's head is generally scanned repeatedly at one location over a short period of time in order to monitor the wash-in and wash-out of an iodinated contrast bolus administered into the peripheral venous circulation. This may result in very high radiation dose (in the order of hundreds of mGy) locally to the skin and the eye lens and can lead to deterministic effects, such as erythema (skin burn) and epilation (hair loss). High dose to the eye lenses may cause cataractogenesis if the eye lenses are directly irradiated. More recent data suggested that the threshold for lens opacities to occur is substantially lower than 2 Gy, if it exists at all.[2]

In order to investigate the radiation dose from CT perfusion scans, it is essential to have dose metrics that are easily obtained. Currently, CTDI is the most widely used dose metric for estimation of CT radiation dose and is reported on almost all CT scanners, and more recently, in patient dose reports, such as that shown in Fig. 1. However, CTDI is not patient dose; instead it represents the radiation dose to a homogeneous cylindrical plastic phantom.[3] In addition, the CTDI calculation assumes a contiguous set of scans over a relatively large region, and the measurements involve the use of a 100 mm long ion chamber, which approximates multiple scan average dose (MSAD) for scans acquired using table increment. While the assumptions behind the CTDI metric fit well to many CT clinical applications, they are not ideal for CT perfusion imaging where there is no table increment, where a relatively narrow swath of tissue is irradiated, and where local peak skin dose and eye lens dose are of greater interest. CTDI has been demonstrated to overestimate the peak skin dose for these reasons.[4]

Thus, it may be more appropriate to use methods described in the American Association of Physicists in Medicine (AAPM) Report No. 111, where measurements are performed under the actual scan mode (e.g., helical or dynamic axial) using a small ion chamber with a shorter active length in longitudinal direction in a long phantom to represent the equilibrium dose.[5] In the context of brain perfusion, AAPM Report No. 111 style measurements are not really equilibrium dose in an extended scan but rather a point dose measurement acquired within the scan range. Therefore, it is appropriate to perform the measurements at 12:00 in a 16 cm phantom to estimate the peak dose. Although AAPM Report No. 111 measurements could potentially provide more accurate dose estimation to peak skin and eye lens dose, this dose estimate method still does not take into account the true complexity or the heterogeneity of a patient's anatomy.

The ImPACT CT organ dose estimation tool, a commonly used tool for determining CT dose, does allow the user to select a specific scan range and report patient dose based on Monte Carlo methods.[6,7] However, while the user can specify scanner output by make and model, modern CT scanner models are approximated or matched to older, originally measured, scanner output data from 1980s. Furthermore, ImPACT uses the MIRD mathematical patient model in which all organs are represented by highly approximated simple geometries in a single hermaphroditic model of a given size and shape. This dose estimation tool also estimates dose to the eye lens, but it does not estimate the peak skin dose from a scan; rather it reports back the average dose to the entire skin, which is not the metric of interest for this exam. Though there are limitations, Monte Carlo based methods simulations using realistic voxelized patient models have been regarded and accepted as the accurate method for the estimation of radiation dose to individual organs.[8–16]

The local dose to skin tissue and the eye lens from CT neuroperfusion scans should be well understood. Previous work has investigated the peak skin dose and eye lens dose during CT neuroperfusion scans for a range of scanning protocols using one patient model.[17]

The purpose of this study is to: (a) expand the scope of the previous work and investigate the effects of patient size on radiation dose from CT neuroperfusion exams using four different adult patient models, and (b) investigate how well these doses can be approximated not only by $CTDI_{vol}$, which is currently reported on scanner consoles, but also by other current or future CT dosimetry tools, such as values derived from the ImPACT dosimetry spreadsheet tool and measurements based on AAPM Report No. 111.

2. METHODS AND MATERIALS

2.A. CT scanners modeled

Four MDCT scanners, including a Siemens Sensation 64 scanner, a Toshiba Aquilion 64 scanner, a Philips Brilliance 64 scanner, and a GE LightSpeed VCT scanner, were modeled to represent a range of models from all four major manufacturers. The Siemens Sensation 64 (Siemens Healthcare, Forcheim Germany) allows kVs of 80, 100, 120, and 140 and with a single bowtie filter. The widest collimation for a neuroperfusion exam with this scanner is 24 × 1.2 mm (28.8 mm

total nominal beam width). The Toshiba Aquilion 64 (Toshiba Medical Systems, Nasu, Japan) offers kVs of 80, 100, 120, and 135 and employs two different bowtie filters. As adult head scans primarily use the small bowtie filter, it was modeled in all our simulations. The widest collimation for a neuroperfusion exam with the Toshiba scanner is 64 × 0.5 mm (32 mm total nominal beam width). The Philips Brilliance 64 (Philips Healthcare, Cleveland, OH) allows kVs of 80, 120, and 140 and one size bowtie filter. The widest collimation for a neuroperfusion exam with this scanner is 32 × 1.25 mm (40 mm total nominal beam width). The GE VCT (GE Healthcare, Waukesha, WI) offers kVs of 80, 100, 120, and 140 and employs three different bowtie filters. The medium sized bowtie is primarily used for head and was modeled in our simulations. The widest collimation for a neuroperfusion exam with this scanner is 64 × 0.625 mm (40 mm total nominal beam width).

2.B. Monte Carlo simulation tools for CT scanners

MCNPX (MCNP eXtended v2.6), a Monte Carlo method based software package developed at the Los Alamos National Laboratory, was used for all simulations in this study.[18,19] The simulations were performed in photon mode (assuming charged-particle equilibrium) with a cutoff energy of 1 keV. The native MCNPX source code (file source.f) was modified to allow for sophisticated source inputs for CT scanners, including the information of spectrum, bowtie filter, table feed, collimation, scan start location, scan length, and so on.[10,11] In order to generate necessary simulation information for specifying x-ray spectrum and bowtie filter, a previously developed methodology was used in this study to construct equivalent CT x-ray sources. The equivalent source method uses data that can be obtained from direct scanner measurements (including half value layer, quarter value layer, and bowtie profile measurements) to generate an equivalent spectrum and bowtie filter profiles for creating CT source models for our Monte Carlo simulations.[20] As stated above, four scanners from the major manufacturers were modeled using this method. These models were validated against measurements in CTDI body and head phantoms at both center and 12:00 positions and all agreed to within 5%.[20]

2.C. Patient models

The GSF (now: Helmholtz Zentrum München) voxelized phantoms are a series of patient phantoms with segmented individual organs and tissues.[21] Of specific interest for this study was that both skin and lens of the eye were explicitly represented in these patient models allowing radiation dose to be specifically tallied in these voxels. Because CTP examinations are rarely performed on pediatric patients, only adult patients were considered in this study. Two adult male and two adult female patient models (Irene, Donna, Golem, and Frank) were selected to represent a reasonable adult patient cohort. As shown in Table I, although these four patient models have body habitus of differing size, their head sizes are very similar. The head perimeter was measured at the level of the eyes for each patient model. The elemental composition and mass density of each organ are required in order to incorporate each phantom into the Monte Carlo simulations and ICRU 44 organ composition tables were used to derive these values.[22]

TABLE I. Age, gender, and size descriptions of the 4 patient models used in this study.

Model	Age (yr)	Gender	Weight (kg)	Height (cm)	Head perimeter (cm)
Golem	38	Male	69	176	61
Frank	48	Male	95	174	61
Irene	32	Female	51	163	57
Donna	40	Female	79	170	56

2.D. Scanning protocol

For each combination of the four patient models and the four scanner models, all available tube potentials were simulated and the doses were reported on a per 100 mAs basis. We realize that appropriate scanning techniques would involve the adjustment of mAs as tube potential is changed, and our results are easily linearly scalable by the actual mAs used for a given scanner and tube potential setting. As in the previous study, the scan simulations were performed using repeated axial scans at the location where the primary beam covers the eye lens completely, to represent a worst case scenario.[17]

The widest collimation and typical bowtie filter for head scans were used for each scanner. It should be noted that although the highest tube voltage setting (140 kV or 135 kV) is not typically used and is not recommended for brain perfusion scans in clinical protocols, they are included in our results for reference.

2.E. Estimation of peak skin dose and eye lens dose

By defining the tally voxels at various locations, the radiation dose can be assessed anywhere in the patient models using MCNPX. In order to get the peak dose for skin, the mesh tally feature in MCNPX was used to get a 3D dose distribution in the patient model within the scan range. Mesh tallies are composed of a 3D array of voxels in a high-resolution Cartesian-coordinate mesh structure. These mesh tally voxels were configured to exactly coincide with the voxels making up the patient phantom.

Since the mesh tally result is a 1D array representing a 3D dose distribution, it does not directly distinguish between different tissues and so further processing is required. In order to identify the skin tissue and the eye lens tissue, a MATLAB subroutine was created to map the original patient model matrix to the 3D dose distribution matrix from the mesh tally. The peak skin dose and eye lens dose were then obtained as the maximum dose and the average dose of those voxels identified as belonging to the skin and eye lens, respectively. The dose results were first divided by the density of the skin or eye lens to convert the unit from MeV/cm^3/particle

to MeV/g/particle, then it was multiplied by normalization factors to get absolute dose. The normalization factors were calculated from scan measurements in air at isocenter and corresponding simulations in air at isocenter, as described in previous publications.[10,11]

2.F. Comparison of estimated peak doses to measurements and ImPACT calculations

In order to investigate how well CTDI and AAPM Report No. 111 measurements predict the peak dose of eye lens and skin, these values were obtained by direct measurements on the scanners themselves. To obtain $CTDI_{vol}$ values, standard CTDI head measurements (a single axial scan with a 100 mm long pencil ion chamber in a 16 cm diameter PMMA CTDI head phantom) were performed using the collimation and bowtie filter settings described above for each scanner and repeated for all available tube voltages at a specified mAs value. Then $CTDI_{vol}$ values (in this case equal to $CTDI_w$) under each condition were calculated according to the weighted summation of CTDI at the 12:00 position and CTDI at the center position[23] and reported on a per 100 mAs basis to account for the effects of the tube current time product.

AAPM Report No. 111 small chamber measurements for single axial scans were also performed and readings from the 12:00 position of a CTDI head phantom were obtained using a small (0.6 cc) ionization chamber (Model 10×5-0.6CT, Radcal Corporation, Duarte, CA); this chamber has an active length of approximately 20 mm. Due to access limitations on the Philips scanner, AAPM Report No. 111 small chamber measurements were only performed for the Siemens Sensation 64 scanner, the GE LightSpeed VCT scanner, and the Toshiba Aquilion 64 scanner. For each available scanner, measurements were performed at all available tube potentials.

Eye lens dose estimates were also obtained for each tube potential setting for all four scanners from ImPACT (version 1.0.3) on a per 100 mAs basis. ImPACT only reports the average dose to the skin instead of local peak dose and as a result only the eye lens doses were compared between Monte Carlo simulation and ImPACT. It should be noted that in ImPACT, the maximum eye lens dose does not occur where the beam is centered over it but instead it occurs at a point slightly more caudal. It is not clear why this is the case; regardless, the scan range was selected so that the maximum eye lens dose was obtained while the eye lens was fully covered by the primary beam. This is illustrated in Fig. 2.[7]

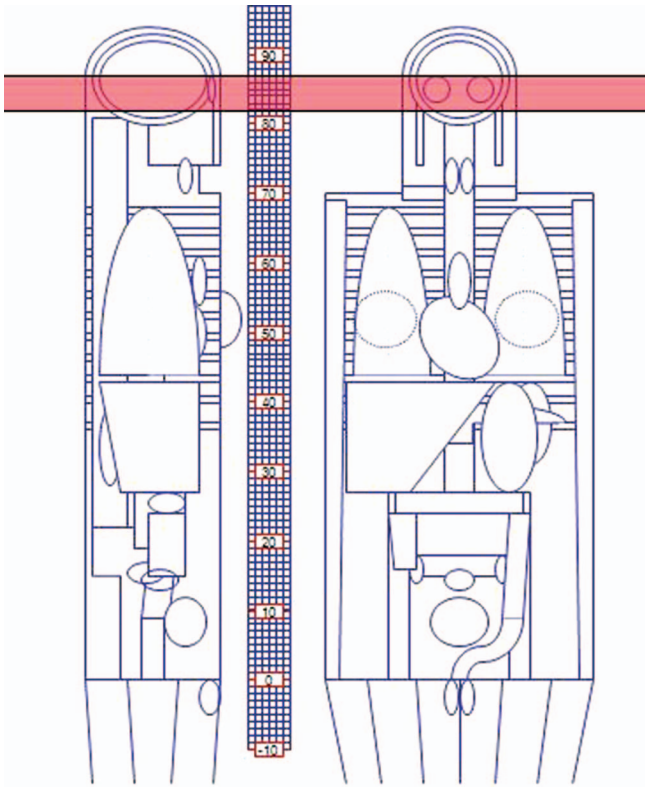

FIG. 2. The mathematical phantom in ImPACT for the calculation of eye lens dose. The shaded region shows a scan range from z = 82 to z = 87 which completely covers the eye lens.

3. RESULTS

3.A. Peak radiation dose to skin and eye lens for different scanners and patients

Table II and Fig. 3 summarize the peak skin dose and eye lens dose results in the unit of milli-Gray (mGy) on a per 100 mAs basis for each tube potential on all four scanners for all four patients. The abscissa of Fig. 3 is the combination of different scanners and patient models, while the ordinate is the radiation dose for different tube potentials. As shown in Fig. 3, peak skin dose is almost always a little higher than eye lens dose under the same condition, and the behaviors of peak skin dose and eye lens dose across different tube potential, different scanners, and different patient models were very similar. Depending on the scanner, tube potential, and patient model, the peak dose to skin from a single CTP examination ranged from 2.3 to 18.2 mGy/100 mAs. For example, the peak skin dose for Irene at 80 kV from Philips Brilliance 64 was 2.3 mGy/100 mAs, while the peak skin dose for Irene at 140 kV from GE LightSpeed VCT was 18.2 mGy/100 mAs. Meanwhile, the dose to the eye lens ranged from 2.0 to 16.2 mGy/100 mAs. For example, the eye lens dose for Donna at 80 kV from Philips Brilliance 64 was 2.0 mGy/100 mAs, while the eye lens dose for Golem at 135 kV from Toshiba Aquilion was 16.2 mGy/100 mAs. It should be noted that 140 kV should not be used in clinical practice for CTP exams; these values are primarily shown for comparison purposes.

The dose difference across various scanners can also be significant and was up to a factor of two for the sample of scanners used in this study (which is consistent with previously published work).[24] For example, for Donna at 120 kV, the peak skin dose from the Toshiba Aquilion64 was 14.2 mGy/100 mAs, while it was 7.3 mGy/100 mAs from the Philips Brilliance 64. This shows that a factor of two difference can exist between two different scanners, even using the same tube potential and mAs settings. This implies that different protocols maybe appropriate for different scanners.

The dose difference across the various patient sizes for a particular scanner was small. For example, for the Siemens

TABLE II. Peak skin dose and eye lens dose from Monte Carlo neuroperfusion simulations for four patient models under all tube potentials on four CT scanners. The doses were normalized on a mGy per 100 mAs basis. (a) Peak skin dose; (b) Eye lens dose.

	Siemens Sensation 64				GE VCT (medium bowtie)				Philips Brilliance 64				Toshiba Aquilion 64 (small bowtie)			
Tube potential	Irene	Frank	Donna	Golem	Irene	Frank	Donna	Golem	Irene	Frank	Donna	Golem	Irene	Frank	Donna	Golem
(a) Peak skin dose (mGy/100mAs)																
80 kV	3.0	2.8	3.0	2.8	5.2	5.0	5.2	4.9	2.3	2.4	2.3	2.4	5.4	5.3	5.4	5.2
100 kV	6.2	6.1	6.3	5.9	8.8	8.5	8.8	8.3	NA	NA	NA	NA	9.5	9.2	9.5	9.0
120 kV	10.5	10.3	10.5	10.0	13.2	12.8	13.1	12.4	7.2	7.5	7.3	7.3	14.1	13.8	14.2	13.4
140 kV (135 for Aquilion CT)	16.4	16.5	16.5	16.0	18.2	17.5	18.1	17.0	11.1	11.6	11.1	11.2	18.1	17.6	18.1	17.1
(b) Eye lens dose (mGy/100mAs)																
80 kV	2.5	2.5	2.2	2.6	4.1	4.3	3.8	4.6	2.2	2.1	2.0	2.3	4.4	4.6	4.0	4.8
100 kV	5.4	5.4	4.8	5.6	7.1	7.5	6.6	7.8	NA	NA	NA	NA	7.7	8.2	7.1	8.5
120 kV	9.3	9.3	8.4	9.6	10.7	11.4	9.9	11.8	6.7	6.8	6.2	7.1	11.5	12.3	10.6	12.7
140 kV (135 for Aquilion CT)	15.0	15.0	13.8	15.6	14.7	15.7	13.6	16.1	10.4	10.4	9.8	11.0	14.7	15.8	13.6	16.2

Sensation at 80 kV, the peak skin dose ranged from 2.8 to 3.0 mGy/100 mAs across all four patient models investigated in this study. These small differences between patients were observed across scanners and tube potentials.

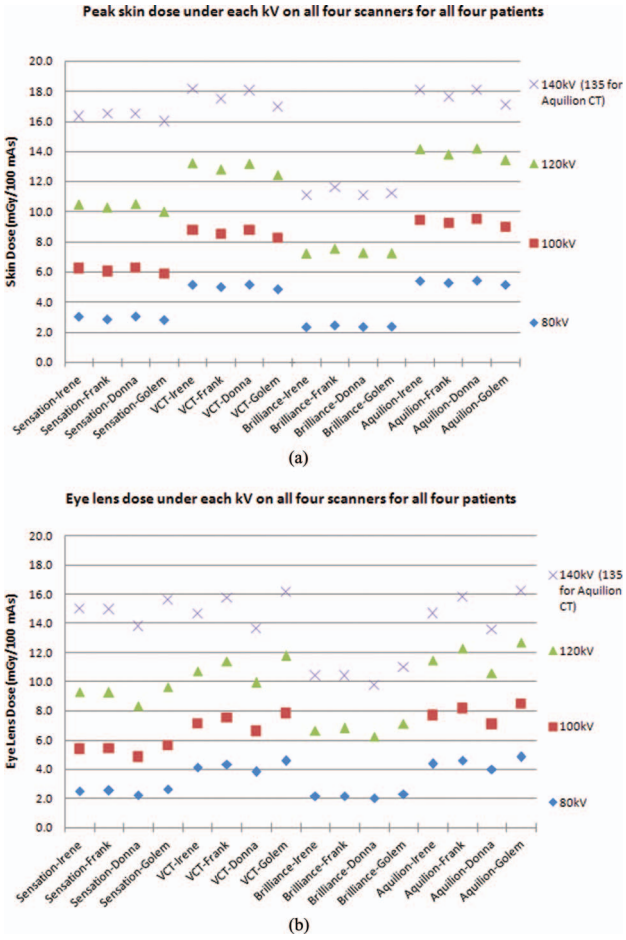

FIG. 3. Simulated peak skin dose (a) and eye lens dose (b) under each tube potential on all four scanners for all four patient models on a per 100 mAs basis.

3.B. Computation time

All the simulations were performed on a parallel computing cluster server with 32 AMD 2.0 GHz processors. The number of particles (NPS) in MCNPX was set to 100 million. The mesh tally used in this study caused prolonged running time because all the photon interactions that happened in each mesh tally voxel had to be tracked. The average running time for each simulation was about 5 h. The statistical error of the results for any given mesh element was within 1%.

3.C. Performance of $CTDI_{vol}$ measurements to predict peak skin and eye lens dose

Table III shows the $CTDI_{vol}$ measurements that were obtained using the 16 cm diameter phantom at the bowtie filtration and collimation settings described above under all available tube potentials on the four scanners modeled in this study. As was done for the simulated peak doses, these values were also normalized on a mGy/100mAs basis. Figure 4(a) shows the ratio of $CTDI_{vol}$ to peak skin dose, while Fig. 4(b) shows the ratio of $CTDI_{vol}$ to eye lens dose for all tube potentials, all scanners, and all patient models. Ratios higher than 1.0 indicate an overestimate by CTDI, while ratio lower than 1.0 indicate an underestimate.

TABLE III. $CTDI_{vol}$ measurements for all kVs on four scanners modeled in this study. The values were normalized on a mGy per 100 mAs basis.

	Siemens Sensation 64	GE VCT (medium bowtie)	Philips Brilliance 64	Toshiba Aquilion 64 (small bowtie)
80 kV	4.0	7.5	3.3	6.9
100 Kv	8.3	13.3	NA	13.2
120 kV	13.7	20.2	11.1	19.9
140 kV (135 for Aquilion CT)	20.9	28.0	16.1	26.5

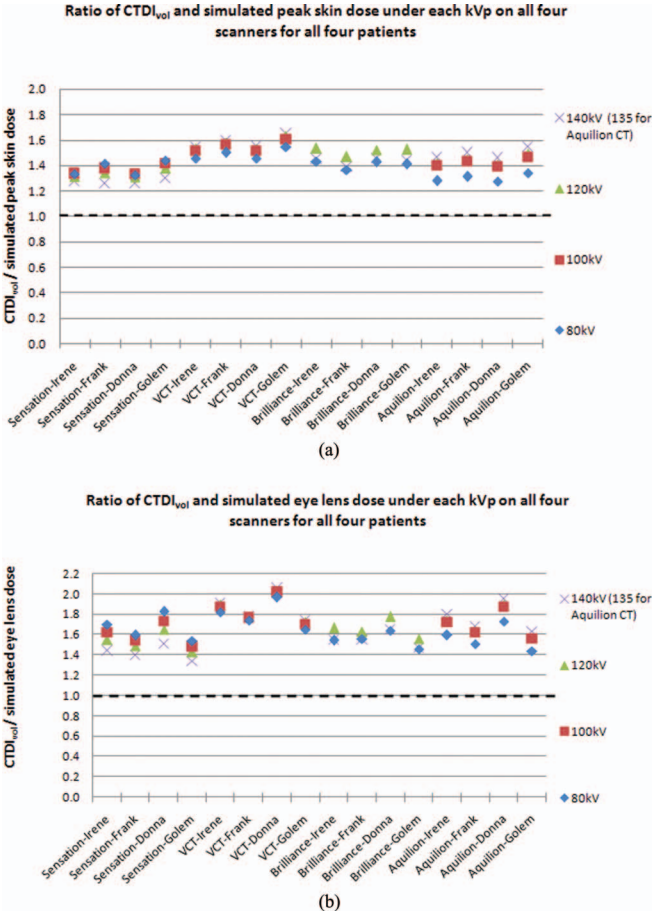

FIG. 4. Over/underestimation of skin dose (a) and eye lens dose (b) when using $CTDI_{vol}$ under each tube potential on all four scanners for all four patient models.

Figure 4 shows that $CTDI_{vol}$ generally overestimates both the peak skin dose and the eye lens dose. Depending on tube potential, the scanner, and patient model, $CTDI_{vol}$ can overestimate the peak skin dose by 26%–65% (average overestimate of 44%), and it overestimates the eye lens dose by 33%–106% (average overestimation of 67%). $CTDI_{vol}$ overestimates the eye lens dose more than the peak skin dose because the eye lens dose (averaged dose for all pixels identified as eye lens) is usually a little lower than the peak skin dose (maximum dose for all pixels identified as skin), as shown in Fig. 3.

3.D. Performance of AAPM Report No. 111 measurements to predict peak skin and eye lens dose

Table IV shows the results of the AAPM Report No. 111 measurements that were performed for three of the four scanners modeled in this study under all tube potential conditions. Figures 5(a) and 5(b) show the ratio of AAPM Report No. 111 measurements to peak skin dose and eye lens dose as estimated using voxelized patient models, respectively. As previously mentioned in Sec. 2.F and noted in Table IV, AAPM Report No. 111 measurements were only performed for three of the four scanners, so Fig. 5 has fewer data points. Figure 5 shows that AAPM Report No. 111 measurements

TABLE IV. AAPM Report No. 111 measurements for all tube potentials on three of the four scanners modeled in this study. The values were normalized on a mGy per 100 mAs basis.

	Siemens Sensation 64	GE VCT (medium bowtie)	Toshiba Aquilion 64 (small bowtie)
80 kV	2.8	6.3	5.4
100 kV	5.6	10.9	9.4
120 kV	9.4	16.5	14.8
140 kV (135 for Aquilion CT)	14.2	22.6	19.1

provided a better predictor than $CTDI_{vol}$ for both peak skin and eye lens dose. Depending on tube potential, scanner, and patient model, AAPM Report No. 111 measurements predicted the skin dose between 14% underestimation and 33% overestimation, with an average overestimation of 7% across all tube potentials, scanner, and patient models. The AAPM Report No. 111 measured values predict the eye lens dose between 9% underestimation and 66% overestimation, with an average overestimation of 27%.

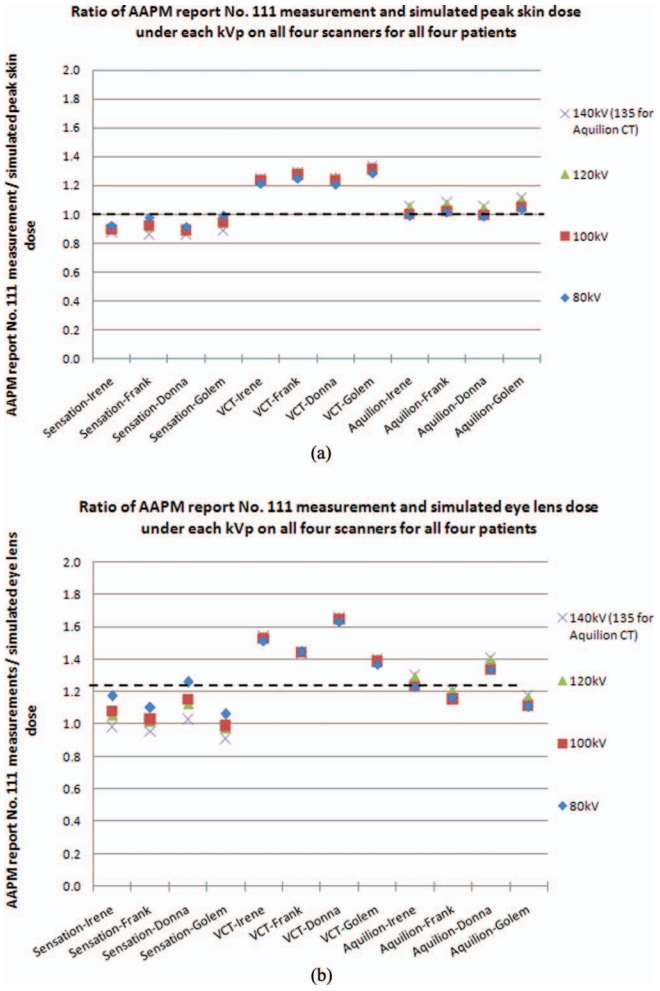

FIG. 5. Over/underestimation of skin dose (a) and eye lens dose (b) using AAPM Report No. 111 under each tube potential on two scanners for all four patient models.

TABLE V. ImPACT eye lens dose calculations for all tube potentials on four scanners modeled in this study. The values were normalized on a mGy per 100 mAs basis.

	Siemens Sensation 64	GE VCT (medium bowtie)	Philips Brilliance 64	Toshiba Aquilion 64 (small bowtie)
80 kV	3.3	6.7	3.2	5.7
100 kV	6.6	12.0	NA	12.0
120 kV	11.0	18.0	9.9	17.0
140 kV (135 for Aquilion CT)	16.0	24.0	13.0	23.0

3.E. Performance of ImPACT calculations to predict eye lens dose

Table V shows the ImPACT calculations for the eye lens dose under each condition. Figure 6 shows the ratios of ImPACT calculations of the eye lens dose to the simulated eye lens dose using Monte Carlo methods. This figure demonstrates that ImPACT calculations also overestimate the eye lens doses in most cases. Depending on the tube potential, the scanner, and patient model, the overestimation can vary from 2% to 82%. The average overestimation was 43%.

4. DISCUSSION AND CONCLUSION

This study used Monte Carlo method based simulations and provided estimates of peak skin dose and eye lens dose from CTP scans for a small range (n = 4) of adult patients under different tube voltage settings for four scanners from major manufacturers. Several dose metrics, including the widely used $CTDI_{vol}$ and the newly proposed AAPM Report No. 111 measurements, as well as ImPACT, a commonly used CT dose tool, were used in this study. Their performances were evaluated as to how well they approximated the peak skin and eye lens doses as determined by voxelized patient specific Monte Carlo models.

Figure 3 provided dose to skin and eye lens at all tube potentials on different scanners for different patients. By comparing the dose differences across tube potential (each column of data points), we demonstrated that at the same mAs, higher tube potential always yields a higher organ dose, as expected.

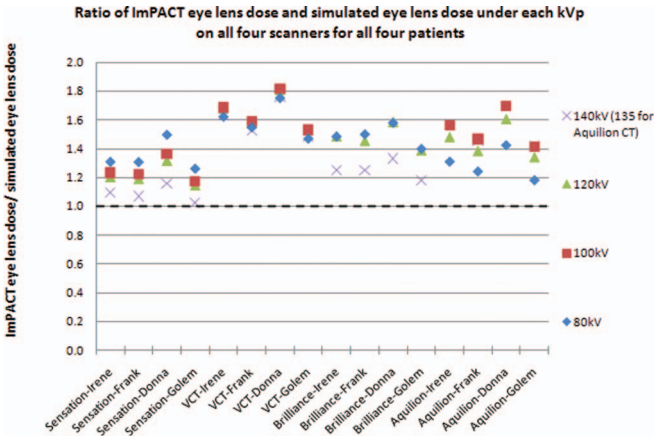

FIG. 6. Over/underestimation of eye lens dose using ImPACT under each tube potential on all four scanners for all four patient models.

By comparing the dose difference across patients, it was shown that the dose variation between patients was very small as expected due to small variations in head size. These results also indicate that the anatomical variation between adult patients is not very large in this sample as far as only the head is considered. The morphologies of both skin and eye lens are reasonably constant across patients: they are both organs located at the surface and have little shielding from surrounding organs.

On the other hand, by comparing the dose differences across scanners, it was shown that there is substantial dose variation among the scanners for a given technique. This is consistent with previous work which studied the doses to different organs in abdominal region and also showed large dose differences.[24] This is primarily because of differences in filtration (including bowtie composition, thickness, and shape) among various CT scanners. However, one cannot assert the superiority of one scanner over another solely based on dose information as image quality across scanners can also differ, requiring different scan protocols. In fact, there are large variations in scan techniques across scanners.

The results reported here can be used to estimate the peak skin dose and eye lens dose from brain perfusion scans for any arbitrary scan protocol using any of the four CT scanners simulated in the study. For example, as illustrated in Table II of a previous study, the skin dose from the AAPM posted protocol for the model Irene ranges from 87 to 348 mGy, and the eye lens dose from the AAPM posted protocol for the model Irene ranges from 81 to 279 mGy.[17]

The results of this study indicate that the $CTDI_{vol}$ overestimates the peak skin dose by between 26% and 65%, and it overestimates eye lens dose by between 33% and 106%. This is primarily because of the integration of the 100 cm long ion chamber in the $CTDI_{vol}$ measurement. It captures (most of) the scatter tails of the longitudinal radiation profile within the length of the 100 cm ion chamber and estimates the average dose to the active volume in the chamber. On the other hand, peak dose in perfusion studies obviously refers to a concept of local dose and should not include the integration aspect of dose determination.

This motivated us to investigate the AAPM Report No. 111 approach which uses a small chamber and provides values closer to a peak dose measurement. Our study demonstrated that this metric does provide a closer estimate to both eye lens and peak skin dose than $CTDI_{vol}$. For example, AAPM Report No. 111 predicts the skin dose between 14% underestimation and 33% overestimation, and it predicts the eye lens dose between 9% underestimation and 66% overestimation. However, it should be noted that if the collimation is narrower than the active length of the small chamber (approximately 20 mm), partial volume correction would be needed; this was not the condition in this study where all collimations exceeded 24 mm. Nonetheless, it does require careful alignment of the phantom and the chamber.

The ImPACT CT dosimetry tool was shown to overestimate the eye lens dose by between 2% and 82%. This may be because ImPACT uses a technique to match the old scanner CT models to the modern CT scanner (based on $CTDI_{vol}$ values) as well as using a geometric patient model, including the eye. It was not possible to estimate peak skin dose using the ImPACT CT dose tool as it only reports the average dose to the entire skin.

Overall, $CTDI_{vol}$ does provide a very conservative overestimate (at least 30%) of peak skin and eye lens dose. Though there is underestimation in some scenarios, predictions using AAPM Report No. 111 measurements provide values that are closer to the simulated values for both eye lens and peak skin dose though it should be noted that this metric is not intended to represent patient dose.

The relative values in Figs. 4 and 5 ($CTDI_{vol}$/peak dose) were shown to be much closer to each other than those in Fig. 3 (peak dose), both across different tube potential within one scanner and across different scanners. This demonstrates that both $CTDI_{vol}$ and AAPM Report No. 111 measurements do a reasonably good job of taking into account the spectra variations across both tube potential and scanners.

It is meaningful to compare these results in three different aspects. First, for a specific scanner and patient model combination, the differences between these relative dose values ($CTDI_{vol}$/peak dose) across tube potentials were small. For example, the points representing different tube potentials in Figs. 4 and 5 almost perfectly overlapped with each other. This indicates that both CTDI and AAPM Report No. 111 dose metrics did take into account the changes of the photon energy spectra; when a different tube potential was used, the behaviors of these two metrics were consistent with the behavior of the simulated organ doses. Therefore, the ratios are almost the same at different tube potentials. Second, for one specific scanner but different patient models, the estimation values did not vary much because the organ doses did not vary much across patients, as described previously. Third, there were some differences among the estimation values from different scanners. For example, for Donna at 80 kV, the $CTDI_{vol}$ overestimation of skin dose was 33% on the Siemens Sensation 64 scanner, 45% on the GE LightSpeed VCT scanner, 43% on the Philips Brilliance 64 scanner, and 28% on the Toshiba Aquilion 64 scanner. These results appear inconsistent with another previously published work where organ dose from helical scans on different scanners was normalized by their $CTDI_{vol}$ and the normalized results were very similar, thus suggesting the feasibility to use the same coefficients to convert $CTDI_{vol}$ to organ dose even for different scanners.[24] The context is a little different in these two studies. In the study by Turner *et al.* helical scans were used, therefore each organ receives not only dose from the primary beam but also scatter radiation contribution from adjacent tube rotations. This is naturally equivalent to the intrinsic property of CTDI measurement, where both primary beam and scatter tails are included in the measured dose. In this study, however, we focused on neuroperfusion scans where axial scans with no table motion are used and there is no scatter radiation contribution from adjacent slices and where the peak skin dose is of interest for deterministic effects. Since the results at different tube potentials have already shown that the photon spectra differences were well taken into account by $CTDI_{vol}$, the differences of $CTDI_{vol}$ comparison to simulation values among these four scanners might be attributed to different collimation efficiency.

Although AAPM Report No. 111 measurements were only performed for three scanners, Fig. 5 showed that their performance was also not very consistent across these three scanners. For example, for the Siemens Sensation 64 scanner and the Toshiba Aquilion 64 scanner, the AAPM Report No. 111 measurements were very close to the simulated peak skin dose, while for the GE LightSpeed VCT scanner, the AAPM Report No. 111 measurements predicted about 30% overestimation relative to simulated values. Since in perfusion studies there is no additional scatter from adjacent rotations in the AAPM Report No. 111 measurements, this dose metric should theoretically provide a more accurate estimate of a point dose. It is unclear why it overestimates the peak dose for the GE LightSpeed VCT scanner. A possible reason is the shape of the bowtie filter since it may affect AAPM Report No. 111 measurements and peak skin dose differently.

In recent years, there has been a trend toward the use of lower tube potential and mA settings to acquire CTP scans. Preliminary data suggests this can be accomplished without adverse impact on lesion conspicuity. This may be a result of a more optimal correlation between the k-edge of Iodine and the scanner settings. The trend is positive, as it provides comparable study diagnostic ability, while achieving significant patient dose reductions. Our results should aid clinicians in understanding the differences and limitations between commonly used dose measurement methods and in optimizing CTP imaging protocols for their particular imaging platform.

There are several limitations in this study. First, it did not model recently developed techniques (wide coverage detectors or volume shuttle mode) utilized in some new scanner models (e.g., Toshiba Aquilion ONE scanner with 16 cm longitudinal coverage, GE Discovery 750HD scanner with jog mode, Siemens Definition Flash scanner, with shuttle mode) during CTP examinations. While this new technique may spread the total dose to a larger volume of the patient's anatomy, it may not necessarily reduce the peak dose, if there is still some overlap between the two beams at same positions, so that a certain part of the anatomy is always irradiated. Second, the sample size of the patient models in our study is not very large. While the four GSF patient models used in this study represent a distribution of patient habitus, they cannot represent the full range population at large. For example, the recently developed ICRP phantoms (ICRP 110)[25] were not used in the study. While these phantoms have higher spatial resolution and may yield more accurate results, this limitation is mitigated by the observation that previous publications have demonstrated that the simulated organ dose results were within 1% between the 256 × 256 and 128 × 128 axial simulation matrix (DeMarco 2007). Therefore, the results from the new ICRP phantoms are not expected to be significantly different than the results from this study. In addition, usually patients with smaller size receive higher organ dose when

the same scanning technique is used.[12,14,15,26] However, only small differences of peak skin and eye lens dose were observed in this study because this study focuses specifically on the patient head region. Third, tube current modulation (TCM) was not explicitly modeled in this study and all the simulations were performed at fixed tube current. Because of the nonuniformity of the attenuation of the patient body across different projection angles, the photon flux reaching the detectors is also not uniform. Therefore, TCM is often suggested to be employed in CT scans to match photon flux on the detectors and, therefore, reduce excessive radiation dose.[27–29] But in CTP examinations, TCM does not modulate tube current greatly because of the relatively circular shape of the head. In fact, it is often not used in these examinations and the AAPM CT protocols for CTP recommend against using it "as it may interfere with the calculation of the BV and BF parameters."[30]

In summary, radiation dose from CT neuroperfusion examinations should be closely monitored. Factors to be monitored include the accurate estimation of radiation dose (including the prospective prediction of dose and the retrospective evaluation of dose), the reduction of patient dose to specific target organs (for example, tilting the gantry or avoiding direct exposure to eye lenses in order to reduce eye lens dose[17]), the optimization of the scan protocol, the enforcement of optimized scan protocols, and the elimination of operator errors. The results of this study could be used to facilitate the optimization of scan protocol by providing very detailed dose perspectives across different patients and scanner models. In addition, it was demonstrated that AAPM Report No. 111 measurements give closer estimates of the peak skin and eye lens dose than $CTDI_{vol}$ values and results from the ImPACT CT dosimetry tool. While AAPM Report No. 111 was only recently published and these measurements are not widely standardized, $CTDI_{vol}$ reported on the scanner can still serve as a conservative estimation of the peak doses. However, one should always be aware that both AAPM Report No. 111 peak dose metric and $CTDI_{vol}$ dose metric are still only indices, instead of actual patient doses.

ACKNOWLEDGMENTS

This work was supported by grant R01EB004898 from the National Institute of Biomedical Imaging and Bioengineering.

[a]Author to whom correspondence should be addressed. Electronic mail: skintchenzhang@gmail.com

[1]K. Miles, J. D. Eastwood, and M. König, *Multidetector Computed Tomography in Cerebrovascular Disease: CT Perfusion Imaging* (Informa Healthcare, Abinfdon, Oxon, 2007).
[2]D. L. Miller, B. A. Schueler, and S. Balter, "New recommendations for occupational radiation protection," J. Am. Coll. Radiol. **9**, 366–368 (2012).
[3]C. H. McCollough *et al.*, "CT dose index(CTDI) and patient dose: They are not the same thing," Radiology **259**, 311–316 (2011).
[4]J. A. Bauhs, T. J. Vrieze, A. N. Primak, M. R. Bruesewitz, and C. H. McCollough, "CT dosimetry: Comparison of measurement techniques and devices," Radiographics **28**, 245–253 (2008).
[5]American Association of Physicists in Medicine, "Comprehensive methodology for the evaluation of radiation dose in x-ray computed tomography," AAPM Report No. 111 (One Physics Ellipse, College Park, MD, 2010).
[6]ImPACT CTDosimetry, "Imaging performance assessment of CT Scanners: A medical devices agency evaluation group. CT scanner matching data, tables of CTDI values in air, CTDIw, and phantom factor values," ImPACT Internet home page: http://www.ImPACTscan.org.
[7]C. Shrimpton *et al.*, *Survey of CT Practice in the UK. Part 2: Dosimetric Aspects. NRPB-R249* (HMSO, London, 1991).
[8]J. J. DeMarco, T. D. Solberg, and J. B. Smathers, "A CT-based Monte Carlo simulation tool for dosimetry planning and analysis," Med. Phys. **25**, 1–11 (1998).
[9]M. Zankl, U. Fill, N. Petoussi-Henss, and D. Regulla, "Organ dose conversion coefficients for external photon irradiation of male and female voxel models," Phys. Med. Biol. **47**, 2367–2385 (2002).
[10]G. Jarry, J. J. DeMarco, U. Beifuss, C. H. Cagnon, and M. F. McNitt-Gray, "A Monte Carlo-based method to estimate radiation dose from spiral CT: From phantom testing to patient-specific models," Phys. Med. Biol. **48**, 2645–2663 (2003).
[11]J. J. DeMarco *et al.*, "A Monte Carlo based method to estimate radiation dose from multidetector CT (MDCT): Cylindrical and anthropomorphic phantoms," Phys. Med. Biol. **50**, 3989–4004 (2005).
[12]J. J. DeMarco *et al.*, "Estimating radiation doses from multidetector CT using Monte Carlo simulations: Effects of different size voxelized patient models on magnitudes of organ and effective dose," Phys. Med. Biol. **52**, 2583–2597 (2007).
[13]E. Angel *et al.*, "Radiation dose to the fetus for pregnant patients undergoing multidetector CT imaging: Monte Carlo simulations estimating fetal dose for a range of gestational age and patient size," Radiology **249**, 220–227 (2008).
[14]E. Angel *et al.*, "Monte Carlo simulations to assess the effects of tube current modulation on breast dose for multidetector CT," Phys. Med. Biol. **54**, 497–512 (2009).
[15]C. Lee *et al.*, "Organ and effective doses in pediatric patients undergoing helical multislice computed tomography examination," Med. Phys. **34**, 1858–1873 (2007).
[16]K. Perisinakis, A. Tzedakis, and J. Damilakis, "On the use of Monte Carlo-derived dosimetric data in the estimation of patient dose from CT examinations," Med. Phys. **35**, 2018–2028 (2008).
[17]D. Zhang *et al.*, "Peak skin and eye lens radiation dose from brain perfusion CT based on Monte Carlo simulation," AJR, Am. J. Roentgenol. **198**, 412–417 (2012).
[18]L. S. Waters, MCNPX User's Manual, Version 2.4.0, Los Alamos National Laboratory Report No. LA-CP-02-408 (2002).
[19]L. S. Waters, MCNPX Version 2.5.C, Los Alamos National Laboratory Report No. LA-UR-03-2202 (2003).
[20]A. C. Turner *et al.*, "A method to generate equivalent energy spectra and filtration models based on measurement for multidetector CT Monte Carlo dosimetry simulations," Med. Phys. **36**, 2154–2164 (2009).
[21]N. Petoussi-Henss, M. Zankl, U. Fill, and D. Regulla, "The GSF family of voxel phantoms," Phys. Med. Biol. **47**, 89–106 (2002).
[22]The International Commission on Radiation Units and Measurements, "Tissue substitutes in radiation dosimetry and measurement," ICRU Report No. 44 (Bethesda, MD, 1989).
[23]M. F. McNitt-Gray, "AAPM/RSNA physics tutorial for residents: Topics in CT. Radiation dose in CT," Radiographics **22**, 1541–1553 (2002).
[24]A. C. Turner *et al.*, "The feasibility of a scanner-independent technique to estimate organ dose from MDCT scans: Using $CTDI_{vol}$ to account for differences between scanners," Med. Phys. **37**, 1816–1825 (2010).
[25]Adult Reference Computational Phantoms, ICRP Publication 110 Ann. ICRP 39 (2), http://www.icrp.org/publication.asp?id=ICRP%20Publication%20110, 2009.
[26]AAPM, "Size-specific dose estimates (SSDE) in pediatric and adult body CT examinations," AAPM Report No. 204, 2011.
[27]M. Gies, W. A. Kalender, H. Wolf, and C. Suess, "Dose reduction in CT by anatomically adapted tube current modulation. I. Simulation studies," Med. Phys. **26**, 2235–2247 (1999).
[28]W. A. Kalender, H. Wolf, and C. Suess, "Dose reduction in CT by anatomically adapted tube current modulation. II. Phantom measurements," Med. Phys. **26**, 2248–2253 (1999).
[29]H. Greess *et al.*, "Dose reduction in computed tomography by attenuation-based on-line modulation of tube current: Evaluation of six anatomical regions," Eur. Radiol. **10**, 391–394 (2000).
[30]AAPM, http://www.aapm.org/pubs/CTProtocols/documents/AdultBrainPerfusionCT.pdf, 2010.